A R C H I V E S O F M E T A L L U R G Y A N D M A T E R I A L S
Volume 53 2008 Issue 1

J. BONARSKI*, J. SMOLIK**, L. TARKOWSKI*, M. BIEL***

# DEPTH-PROFILE OF RESIDUAL STRESSES IN METALLIC/CERAMIC COATINGS

# GŁĘBOKOŚCIOWY PROFIL NAPRĘŻEŃ WŁASNYCH W POWŁOKACH METALICZNO CERAMICZNYCH

The use of X-ray diffraction techniques provides the wide possibilities of applying non destructive tensometry, especially for coatings and near-surface layers. It consists in control of residual stresses arising after different technologies or exploitation conditions. In this paper the "$\sin^2\psi$" method of X-ray stress measurement applied to analysis of its depth profile in Cr, and CrN/Cr coatings is presented. Explanation of physical origins of the stresses revealed by carried out experiments and prediction of the stress evolution in the examined coatings are discussed.

Technika dyfrakcji rentgenowskiej dostarcza szerokich możliwości stosowania nieniszczącej tensometrii, szczególnie w powłokach materiałowych i warstwach przypowierzchniowych. Polega ona na kontroli naprężeń własnych powstających po różnego rodzaju procesach technologicznych jak i w wyniku eksploatacji. W niniejszym artykule zaprezentowano rentgenowską metodę "$\sin^2\psi$" pomiaru naprężeń w zastosowaniu do analizy ich profilu głębokościowego w powłokach Cr i CrN/Cr. Przedyskutowano fizyczne uwarunkowania generowanych naprężeń na podstawie wykonanych doświadczeń i przewidywanego rozwoju naprężeń w badanych powłokach.

## 1. Introduction

For a long time, mutual influence of substrate and coatings or material bulk and a modified near surface layer on state of its structure belong to the most interesting problem from the both research an application viewpoints. The reason is a special, non-homogeneous character of structure of the specific area, which has a crucial meaning for physical properties of material (composition) with layered structure. Besides the material properties, also the structure feature (spatial arrangement of grains) and its state (presence of residual stresses) are significant for durability of such system. Among the structure characteristics essentially influenced on the properties and simultaneously not satisfactorily recognized is configuration of field of the residual stresses.

There are several known ways for determination of residual stresses, such as the destructive mechanical removal layers, methods based on measurement of material properties affected by stresses (ultrasonic techniques, registration of Barkhausen magnetic noise, Raman spectroscopy) and diffraction technique based on measurement of strain of crystallographic lattice. A big advantage of the diffraction technique is its non-destructive character as well as a possibility of macro- and microscale analysis of stress in multi-layer and multiphase materials. A subtle system of stresses, crystallographic texture and/or phase composition accompanied usually the layered structures with interface areas make the material difficult to investigation. For that reason a non-destructive examination ways are required.

Advanced experimental techniques as well as sophisticated method of data processing allow revealing – to some extent – the complicated and still not enough recognized specific nature of the near-interphase areas. Recently developed ways of evaluation of residual stresses or texture analysis of the near-surface area, like a Grazing Incidence Diffraction method [1] or X ray Texture Tomography [2], respectively are sufficient research tools in this field.

As for tensometric procedures revealing a depth profile of the residual stresses, they based on the X-ray and neutron diffraction techniques. Independently of the research tool, problem of result authority and possibili-

* INSTITUTE OF METALLURGY AND MATERIALS SCIENCE, POLISH ACADEMY OF SCIENCES, 30-059 KRAKÓW, 25 REYMONTA STR., POLAND
** INSTITUTE FOR SUSTAINABLE TECHNOLOGIES – NATIONAL RESEARCH INSTITUTE, DEPT. OF SURFACE ENGINEERING, RADOM, 6/10 PUŁASKIEGO STR., POLAND
*** DELPHI POLAND S.A., KRAKÓW, 2 PODGÓRKI TYNIECKIE STR. 2, POLAND

ty of verification of the identified stress level are still open.

The present work describes an attempt of verification of configuration of the stress field remain in chosen coatings of Cr and CrN deposited on structural steel which are one of the most widely applied materials with layer structure.

According to numerous literature records [3–7], multilayer Cr-CrN coatings are characterised by a very good crystallographic matching of subsequent constituent Cr and CrN layers [3] and by the creation of crystalline transient layer with the thickness of tens nanometers [7]. It ensures a good connectivity of layer in particular separation zones, and as a result, good maintenance properties: adhesion [4], abrasive wear resistance [5] and corrosive resistance [6]. By M. Berger at al. [8] has also been revealed that the presence of constituent layers with a greater plasticity in the multilayer coating significantly increases coating's abrasive wear resistance. The outcomes of experimental testing indicate in this case an important role of constituent layers of metallic chromium, which thanks to their capability of plastic deformation, limit the operation of hard particles in the friction area.

The goal of presented stress analysis is comprehensive characterization of material structure, essential from viewpoint of prediction it behaviour in exploitation conditions. Based on experimental data, a large diversity of the stress profile have had been identified. Applied measurement way, data processing and interpretation of results are the subject of the work.

## 2. Material

Three various metallic coatings deposited by different methods on steel substrate previously heat-treated or/and nitraded was subdued to investigation:

**Cr coating** (ca. 25 μm thick) has been deposited by a galvanic method on a steel rod of 22 mm diameter with hardend (martensitic) near-surface layer of 2 mm thick (Fig. 1). Three samples of the Cr coated on steel rod in different technological conditions denoted as Cr1, Cr2 and Cr3 were examined.

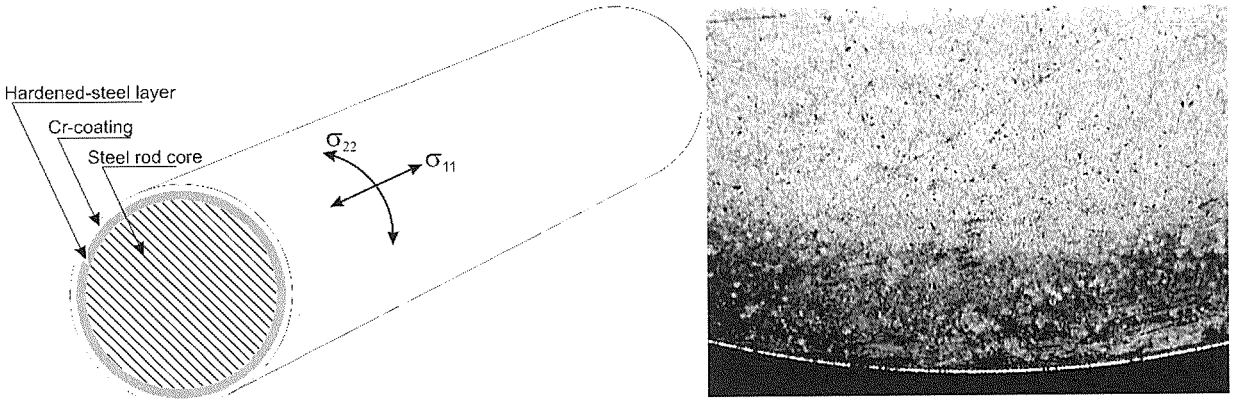


Fig. 1. Scheme of steel rod (22 mm diameter) with hardened near-surface layer, coated by Cr (left) and microstructure of its cross section (right)

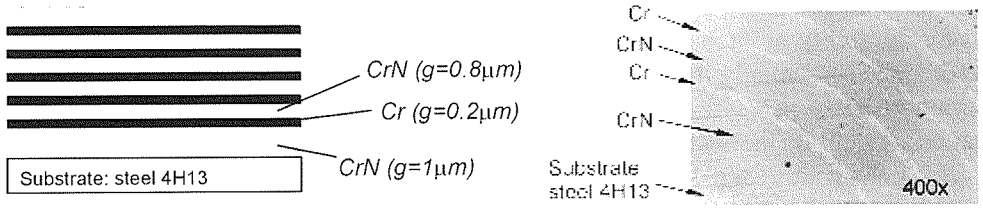


Fig. 2. Scheme (left) and microscope view (right) of structure of multilayer coating Cr-CrN. Thickness of individual layers (denoted as "g") is given in the brackets

TABLE 1

Technological parameters of manufacturing constituent layers materials Cr, CrN in the investigated multilayer coatings

| Material | Atmosphere | Pressure p[mbar] | Polarisation voltage Ubias [V] | Foundation temperature T [°C] | Deposition speed V [nm/min] |
|---|---|---|---|---|---|
| Cr | 100% Ar | $3.0\times10^{-5}$ | −50 | 450 | 50 |
| CrN | 100% $N_2$ | $3.5\times10^{-2}$ | −200 | 450 | 60 |

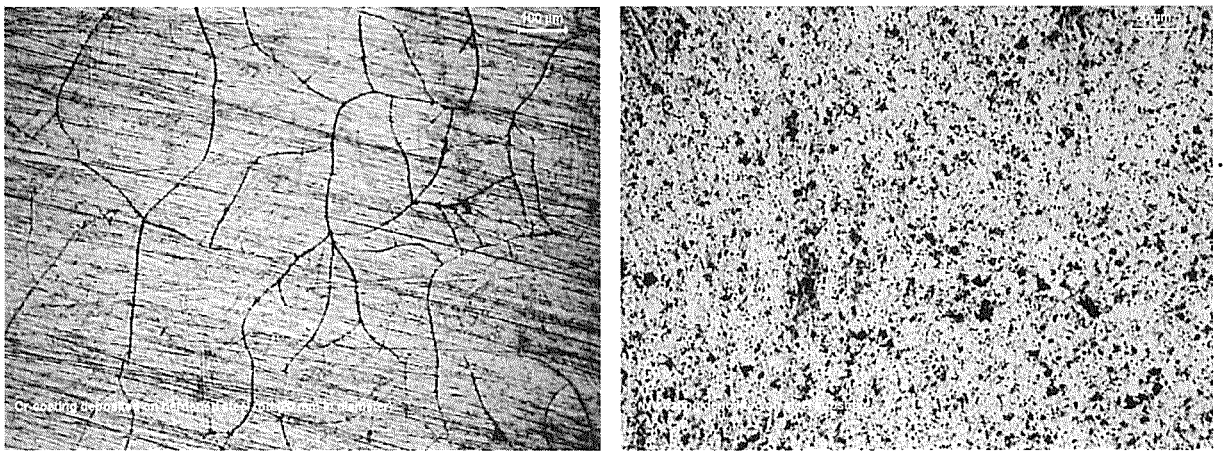

Fig. 3. Microstructure of side surfaces of the examined Cr (left) and CrN (right) coating

**CrN and multilayer Cr-CrN coatings** based on chromium nitride were obtained at Plasma Technology Centre ITE-PIB in Radom by means of arc-vacuum method [9, 10] with the use of MZ383 device by Metaplas Ionon company.

The CrN coating ca. 6 μm thick was deposited on 4H13 steel substrate. In the case of the Cr CrN multilayer coating the following scheme of reciprocal system of particular constituent layers was applied: the first constituent layer deposited directly on the substrate was CrN 1 μm thick. As next 5 two-layer Cr-CrN complexes were deposited, in which Cr thickness amounts to 0.2 μm and the thickness of CrN is 0.8 μm (Fig. 2).

The differentiation of thickness in the manufactured constituent layers was achieved by choosing the deposition process time. Multilayer coatings selected for the stress examination were obtained according to parameters given in Tab. 1.

**Microstructure of** surface of the examined Cr and CrN coatings observed by means of optical and scanning electron microscopy techniques, respectively is presented in Fig. 3.

## 3. Experiments and metodology

Examination of residual stresses was performed by a $\sin^2\psi$ method [11] based on X-ray diffraction data. Respecting the material of substrate and coating of examined samples, the both CoKα and CuKα series of radiation have been applied. For each of the samples, averaged lattice strains were measured traditionally in two mutually perpendicular planes and additionally, the depth profile of it in one of the planes have been investigated.

Values of residual stresses were calculated regarding the isotropic elastic constants calculated by the Reuss model [12, 13] using a computer program *Stress* by Baczmański [14]. Appropriate values of Young's modulus, Poisson's ratio and isotropic diffraction elastic constants $s_1$, $\frac{1}{2}s_2$ were taken from literature data [15] and given in Tab. 2.

TABLE 2

Elastic constants of examined materials

| Parameter | | Material | | |
|---|---|---|---|---|
| | | Cr | CrN | α-Fe (Martensite) |
| *Young's modulus* | E [GPa] | 279 | 216 | 201 |
| *Poisson's ratio* | ν | 0.21 | 0.20 | 0.296 |
| *Diffraction elastic constants* | $s_1$ [1/TP] | −0.75 | −0.97 | −1.47 |
| *Diffraction elastic constants* | $\frac{1}{2}s_2$ [1/TP] | 4.34 | 11.20 | 6.43 |

Measurement apparatus equipped with Euler cradle and a parallel X-ray beam optics have enabled to real-

ize a various tilting the sample, its rotation and x y z positioning needed in depth-profile analysis of residual stresses. Besides of sample tilting by the $\psi$ angle imposed by the $\sin^2\psi$ method another one by the $\chi$ angle was applied to changing the penetration depth of X ray beam during the measurement [2].

As a result, the diffraction effects could be registered for thicker and thicker (counting from outer surface of sample) layers of material. For such chosen successive layers of $L$ thickness (Fig. 4) the residual stresses $\sigma^{(L)}$ have been calculated by $\sin^2\psi$ procedure. Then using a simple proportion between the thickness of successive layers and regarding exponentional character of attenuation of the intensity of X ray beam due to absorption, values of the stresses ascribed to individual sub-layers of $sl$ thickness (denoted as $\sigma^{(sl)}$) have been evaluated as follows.

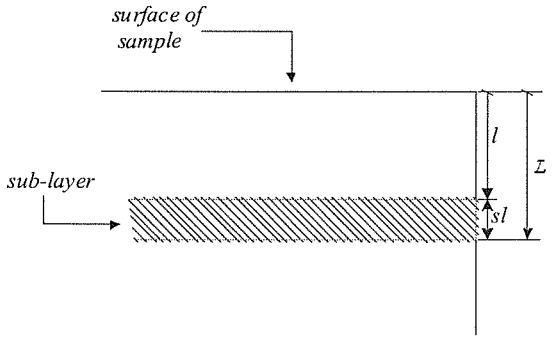


Fig. 4. Scheme of layers considered at measurement and calculating procedures heading to reveal the depth-profile of residual stresses

The averaged $\sigma^{(L)}$ component of the stress in the measured near-surface layer of sample with $L$ thickness is a superposition of the $\sigma^{(sl)}$ and $\sigma^{(l)}$ stresses existed in a chosen sub layer ($sl$) and in whole material ($l$) layer laying directly above of it, respectively (see Fig. 4). Analogously to procedure of separation of a sub-layer signal contained in diffracted beam applied in the X-ray texture tomography [2], following relation can be introduced:

$$\sigma^{(L)} = (1 - A) \cdot \sigma^{(l)} + A \cdot \sigma^{(sl)}, \tag{1}$$

where the factor $A \in (0, 1)$ defines the proportion (weight) between the stresses existed in the near surface layer ($l$) and under near surface one separated from the whole depth of examined volume ($L$). After transformation the Eq. (1), interesting values of the $\sigma^{(sl)}$ stress can be calculated by following equation:

$$\sigma^{(sl)} = \frac{1}{A}\left(\sigma^{(L)} - (1 - A) \cdot \sigma^{(l)}\right) \tag{2}$$

The near surface layer acts as a sort of filter attenuating the intensity of the beam passing through the part of sample. This weakening expressed by the $A$ parameter in Eq. 1 can be described by means of Beer-Lambert's absorption law, which, after taking into consideration the definition of the effective penetration depth in the applied a non-symmetrical focusing geometry of measurement can be expressed as follows [2]:

$$A = e^{-\mu \cdot \xi \cdot L} \tag{3}$$

where $\mu$ is linear absorption coefficient of examined material for applied radiation, and $\zeta$ (here $6 < \zeta < 10$) is scaling parameter represents the geometrical dependence between the angles $(\theta, \omega, \chi)$ defining the sample position in the goniometer during the measurement of diffraction effects from near-surface layer with a given thickness [2]:

$$\xi = \frac{\sin(\theta - \omega) + \sin(\theta + \omega)}{\sin(\theta + \omega) \cdot \sin(\theta - \omega)} \cdot \frac{1}{\cos\chi} \tag{4a}$$

All measurements presented in this work were made at $\omega = 0$ geometrical condition so the above relation can be simplified:

$$\xi = \frac{2\sin\theta}{\sin^2\theta} \cdot \frac{1}{\cos\chi} \tag{4b}$$

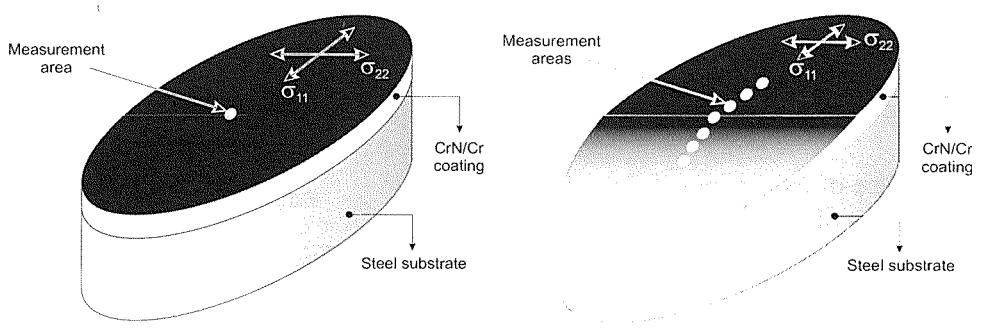


Fig. 5. Scheme of samples with deposited mono- CrN and multilayer Cr-CrN coatings (left) and additionally examined oblique section (right) with marked localization of measurement areas of residual stresses

Subsequent values of the $\sigma^{(sl)}$ component of the stresses depth profile were calculated by Eq. (2) based on the $\sigma^{(L)}$ and $\sigma^{(l)}$ ones obtained in individual measurements with controlling depth by means of $\chi$-tilting of sample ($\chi \neq 0$). Resulted depth-profiles for the Cr, CrN and Cr-CrN coatings are presented in Figs. 6 and 7, respectively. Additionally, in the case of the CrN and Cr-CrN coatings traditional stress analysis by the $\sin^2\psi$ method was performed on a special oblique section as it is shown in Fig. 5. In this way a comparison of traditional and the suggested manners of revealing the detph-profile of stresses has been gotten.

## 4. Results and its discussion

Averaged level of residual stresses revealed in the examined coatings and substrate materials by conventional $\sin^2\psi$ method (at $\chi = 0$) are given in Tab. 3. All identified values indicate a compressive character of the stresses.

In the case of the Cr coatings the results are related to the border circumference lying in a plane of cross-section of the rods, marked in Fig. 1 as $\sigma_{22}$ component of the stress field. Obtained results reflect an average level of residual stresses in outer zone of the Cr coatings (ca. 6.2 μm thick) and the substrate steel (whole matrensitic layer visible eg. in Fig. 1). Relatively higher level of the stresses is noticed for Cr3 and essentially lower ones for Cr2 and Cr1 samples.

Among the CrN and Cr-CrN coatings the second one manifests essentially higher averaged level of residual stress. Substrates of the both layers are stressed similarly at level of −750 MPa. As it was examined, the coatings and it substrates exhibit similar level of residual stresses measured in two mutually perpendicular planes, i.e. $\sigma_{11} \neq \sigma_{22}$.

Depth-profiles of the $\sigma_{22}$ component of stresses were obtained by means of non-standard measurement geometry described above (at $\chi \neq 0$) and calculation by the $\sin^2\psi$ method regarding Eq. (2). Depth-profile of the same stress component reveals its local level to some depth form surface to the coating-substrate interface.

TABLE 3

Averaged values of residual stresses identified in examined sections of the samples

| Sample (coating) | Orientation of identified component of stress field | | Level of stresses [MPa] | |
|---|---|---|---|---|
| | Plane | Direction | Coating | Substrate |
| Cr1 | Cross-section of rod | Border circumference | −516 ± 205 | 508 ± 43 |
| Cr2 | Cross-section of rod | Border circumference | −652 ± 205 | — |
| Cr3 | Cross-section of rod | Border circumference | −1590 ± 205 | 944 ± 45 |
| CrN | Surface of coating | Arbitrarily chosen | −1254 ± 53 | −750 ± 45 |
| Cr-CrN | Surface of coating | Arbitrarily chosen | −1807 ± 60 | −750 ± 45 |

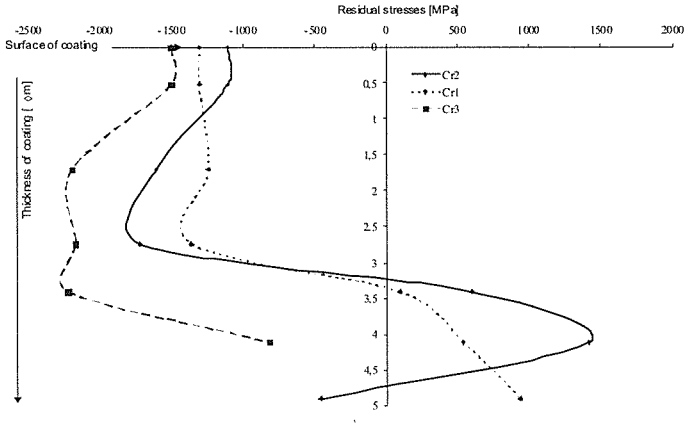


Fig. 6. Depth-profiles of residual stresses ($\sigma_{22}$ component) in examined monolayer Cr coatings (Cr1, Cr2 and Cr3) related to the border circumstance laying in a plane of cross-section of the rods

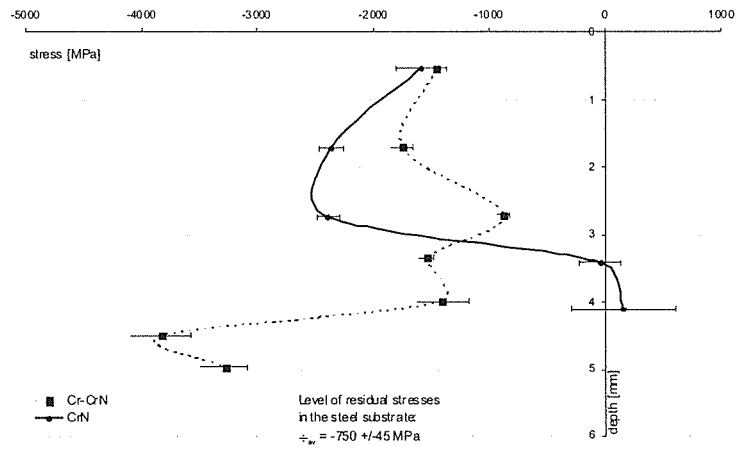


Fig. 7. Depth-profiles of residual stresses ($\sigma_{22}$ component) in examined CrN and multilayer Cr-CrN coatings related to arbitrarily chosen plane perpendicular to outer surface of the sample (marked grey area indicate the level of stresses in substrate)

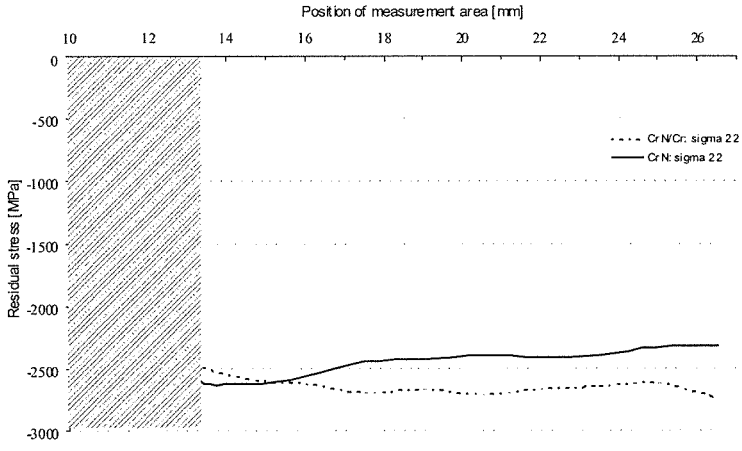


Fig. 8. Distribution of value of the $\sigma_{22}$ stress component in the slanting section shown in Fig. 5 for the both Cr and Cr-CrN coatings (shaded range consists the results charged by big errors due to the substrate artefacts in registered diffraction profiles, and should be omitted)

In the case of the Cr coatings (Fig. 6) the profiles reach to depth ca. 5.0 μm characterizes significant changes of values. It concerns especially to sample Cr1 and Cr2 for which below 3.0 μm the stresses change its sign ("–" → "+") from compressive becoming extensive. Such a change has no noticed in coating Cr3.

In the case of CrN and Cr CrN coatings, suitable gradients of stress are presented in Fig. 7. As it can be noticed, the stresses change strongly with distance from the sample surface. In the case of monolayer CrN, the change of sign was identified even. It has consequences in behaviour or the coating during exploitation. Comparing the two kinds of coatings, the Cr-CrN one is essentially more durable when compared to the CrN. The reason is in stress-extenuating influence of the Cr inter layers which was identified in the presented depth-profile (see Fig. 7).

Results of a stress topography of the $\sigma_{22}$ component registered in the oblique section (see Fig. 5) for the both Cr and Cr-CrN samples are given in Fig. 8. The results shown that distribution of the stresses measured at different depth of coatings after it sectioning have a similar character and are definitely different when compared to its depth-profile registered in non-destructive manner. Moreover, based on the results presented in Fig. 8 interpretation of significant differences in exploitation properties of the both kind of coatings becomes greatly difficult.

It is worth noticing that yield stress ($R_e$) of the Cr or CrN coating depends essentially on its thickness and

can be vary in the broad limits. The limits in the case of the CrN is a hundreds to a few thousands MPa, and for that reason the identified maximum values of the stresses seems to be reasonable high (see Fig. 8).

## 5. Summary

Stress in coatings is mainly the net sum of tensile/compressive stresses due to incompatibility at the grain boundaries and in the near-substrate area. Resultant components leads to a stress gradient, like in the examined coatings of Cr and Cr-CrN.

The values of stresses identified in two mutually perpendicular planes denoted as $\sigma_{11}$ and $\sigma_{22}$ allow to recognize an anizotropy of the field of residual stresses existed in examined coatings.

Depth-profiles of the $\sigma_{22}$ component of stresses presented in Figs. 6 and 7 are much more informative when compared to its averaged level obtained in conventional $\sin^2\psi$ method. At first the depth-profile reveals configuration of the stress field versus surface or interface distance and indicates localization of potential destruction area. It has an essential meaning in designing the mono- and multilayer coatings and in analysis of deterioration of material structure in exploitation conditions.

Obtained result show that the averaged level of stresses do not express the stress state of such a structure like coatings and near-surface layers. As long as the gradient of the stresses (at least one component of it) is unknown, the "stress picture" of material is greatly insufficient. In the case of significant anisotropy of the stress field, its interpretation based on one, averaged value only can be – to some extent – even erroneous. Presented in the work the non-destructive manner of revealing the depth-profile is greatly effective in reference to the metallic/ceramic coatings when compared to classical mode of stress analysis on sections.

**Acknowledgements**

The authors wish to thank Eng. St. Kotas for his assistance in stress examination and Dr. M. Faryna for his help in microstructure observation. The work was financially supported by the State Committee for Scientific Research as the PW-004/ITE/07/2005 and Nr 3 T08C 064 26 research grants.

*Received: 3 December 2007.*

REFERENCES

[1] S.J. Skrzypek, A. Baczmański, W. Ratuszek, E. Kusior, New approach to stress analysis based on grazing-incidence X-ray diffraction, Journal of Applied Crystallography **34**, 427-435 (2001).

[2] J.T. soBonarski, X-ray texture tomography of near surface areas, Progress in Materials Science **51**, 61-149.

[3] J. Romero, J. Esteve, A. Lousto, Period dependence of hardness and microstructure on nanometric Cr/CrN multilayers, Surface and Coatings Technology **188-189**, 338 (2004) .

[4] L. Major, et al., Crystallographic aspects related to advanced tribological multilayers of Cr/CrN and Ti/TiN types produced by pulsed laser deposition (PLD), Surface and Coatings Technology **200**, 6190 (2006).

[5] M. Berger, U. Wiklund, M. Eriksson, H. Engqvist, S. Jacobson, The multilayer effect in abrasion – optimising the combination of hard and tough phases, Surface and Coatings Technology **116-119**, 1138 (1999).

[6] H.A. Jehn, Improvement of the corrosion resistance of PVD hard coating-substrate system, Surface and Coatings Technology **125**, 212 (2000).

[7] S. Han, et al., The effect of Cr interlayer on the microstructure of CrN coatings on steel, Thin Solid Films **377-388**, 578 (2000).

[8] M. Berger, U. Wiklund, M. Eriksson, H. Engqvist, S. Jacobson, The multilayer effect in abrasion-optimising the combination of hard and tough phases, Surface and Coatings Technology **116-119**, 1138 (1999).

[9] M. Mack, Surface technology. Wear protection. Verlag moderne industrie AG&Co D-8910 Landsberg/Lech, Box 1751.

[10] R.F. Bunshah, Deposition Technologies for Films and Coatings, NOYES PUBLICATIONS, Park Ridge, New Jersey, USA.

[11] I.C. Noyan, J.B. Cohen, Residual Stresses – Measurement by Diffraction and Interpretation, Springer-Verlag, Berlin (1987).

[12] A. Reuss, Berechnung der Fliessgenze von Mischkristallen auf Grund der Plastizitätsbedingung für Einkristalle, A. Angew. Math. Mech. **9**, 49 (1929).

[13] A. Baczmański, Stress field in polycrystalline materials studied using diffraction and self-consistent modeling, Thesis, AGH UST, Kraków (2005).

[14] A. Baczmański, Program Stressfit, AGH (2004).

[15] G. Simmons, H. Wang, Single Crystal Elastic Constant and Calculated Aggregate Properties, The M.I.T Press (1971).